Computational Optimization of Vacuum Swing Adsorption Processes for CO_2 Capture Using MUF-16

Elnaz Jangodaz[a,b,*], Shane G. Telfer[a,b]

[a]*MacDiarmid Institute for Advanced Materials and Nanotechnology, School of Food Technology and Natural Sciences, Massey University, Palmerston North 4410, New Zealand.*
[b]*Captivate Technology Ltd, Palmerston North 4410, New Zealand.*

Abstract

MUF-16 (MUF = Massey University Framework) is an excellent adsorbent for CO_2 capture that is being commercialized by Captivate Technology to address point-source emissions. It is a porous metal-organic framework (MOF) that has a high selectivity for CO_2 over nitrogen and methane, tolerance to impurities and long-term stability. It can be manufactured on a large scale from inexpensive precursors. This work highlights the effectiveness of MUF-16 for high-performance carbon dioxide capture from flue gases with high purity and low energy requirements.

Finding the optimal operating conditions for implementing MUF-16 in vacuum swing adsorption (VSA) process through experiments is a challenging and time-consuming task. Instead, numerical simulations are generally used. For this purpose, we developed a multi-objective optimization model in MATLAB. We carried out numerical optimization of the VSA process for post-combustion CO_2 capture from dry flue gases. Fundamental characteristics of MUF-16 were first evaluated by adsorption isotherms, kinetic measurements, and breakthrough curve experiments. Suitable isotherm and adsorption rate models were applied to the experimental data to determine the CO_2 and N_2 adsorption isotherm and kinetic parameters of the adsorbent. Model validation was performed by comparing the simulation results for breakthrough with relevant experimental data on a PVSA unit with 2 kg of adsorbent. Three different adsorption configurations were simulated: a 2-column VSA process with 3, 4 or 5 steps. These configurations were optimized to achieve high CO_2 purity ($\geq 95\%$) and recovery ($\geq 90\%$), while maintaining low energy consumption and high productivity. Each simulation then resulted in Pareto charts for purity, recovery and other parameters. Excellent results were achieved using a simple five-step cyclic process. A parametric study was also carried out to analyze the effect of CO_2 concentration on the Pareto curves. The results confirm the considerable potential of MUF-16 for practical separations of CO_2 from flue gases on an industrial scale.

Keywords: CO_2 capture; MUF-16; Metal-organic framework; Adsorption process simulation; Optimization; VSA; Flue gas

---

* Corresponding author. Email address: e.jangodaz@massey.ac.nz

Nomenclature

Roman symbols		Abbreviations, subscripts and superscripts	
t	time [s]	ADS	adsorption
P	pressure [bar]	BD	CoC blowdown
v	interstitial velocity [m/s]	EVAC	CnC evacuation
p	pressure [pa]	P	pressurization
ΔU	internal energy [kJ/mol]	HR	heavy reflux
y	mole fraction [%]	i	component
T	temperature [K]		
R	universal gas constant [Pa m^3 mol^{-1} K^{-1}]	Greek symbol	
b_o	adsorption equilibrium constant [1/pa]		
$q*$	equilibrium solid phase loading [mol/kg]	ß	heavy reflux ratio
q^{sat}	solid phase saturation capacity [mol/kg]		

1. Introduction

CO_2 is the main contributor to global warming, so reducing CO_2 emissions from industrial processes is crucial [1]. Currently, there are various methods available for CO_2 capture including absorption, adsorption, membrane, and cryogenic separation technologies [2-5]. Choosing the correct technologies for different industrial emission sources is crucial for achieving high efficiencies [6].

Amine absorption, the most mature technology for CO_2 capture, suffers from high energy penalties in the recycling step negative environmental impacts, degradation and corrosion [7]. Adsorption processes using solid-state materials are promising alternatives. They offer advantages such as lower costs due to mild regeneration, ease of handling, and environmental benefits [1, 3]. Vacuum swing adsorption (VSA) is an established technology for separating gas mixtures using solid-state adsorbents in a continuous, cyclic process [8, 9]. Its versatility means that it can be extended to CO_2 capture from various emission streams [10, 11].

Various types of porous solid adsorbents have been extensively studied for CO_2 capture, such as activated carbons, zeolites, and silicon-based materials [12]. More recently, metal-organic frameworks (MOFs) have proven to be excellent materials [13, 14]. The diversity and unique properties of MOFs make them stand out compared to traditional porous materials. Computational methods have greatly accelerated the assessment of MOFs and other adsorbents in pressure-swing processes [11, 15].

The pores of MOFs capture CO_2 by physisorption; thus, release of the CO_2 is inherently a low energy process, Te pores can be specifically designed to have high affinities for target gases, making them highly selective. In addition, certain MOFs are tolerant of water vapour and other contaminants and exhibit rapid adsorption and desorption kinetics. MUF-16 [16-18], a new adsorbent being commercialized by Captivate Technology, is one such high-performance adsorbent that has a high affinity for CO_2 and a low affinity for many other gases such as methane and nitrogen. MUF-16 (MUF = Massey University Framework) has many other attractive characteristics: it is inexpensive and simple to prepare, it is tolerant of gases such as CO, H_2S, NO_x and SO_x, steam, and water vapor, it is thermally stable, and it can be recycled by desorbing captured CO_2 in a straightforward way.

This work highlights the effectiveness of MUF-16 which is currently being commercialized by Captivate Technology [19] for efficient carbon dioxide capture from flue gases on large scale with a low energy penalty.

2. Materials and methods

2.1. Materials

The material studied in this study is MUF-16 (Co(Haip)$_2$), which comprises an inorganic cobalt(II) chain linked by 5-aminoisophthalic acid ligands, Haip [16, 17]. This MOF has pores that enable selective interactions with CO_2 molecules, underlying a strong preference for this gas over N_2, CH_4, and many other small molecules. MUF-16 can be pelletized using a small amount of an appropriate binder and formed into millimetre-scale spherical beads or cylindrical pellets [17].

2.2. Adsorption isotherms

CO_2 and N_2 adsorption isotherms were measured over a pressure range of 0 to 1 bar at six different temperatures to account for temperature dependency in the modelling process (Fig. 1b). The collected data were fitted using a Single-Site Langmuir model (Eq. 1, Table 1) [20].

$$q^* = \frac{q^{sat}bp}{1 + bp}$$

(1)

Table 1. Single-site Langmuir isotherm parameters for the adsorption of CO_2 and N_2 by MUF-16

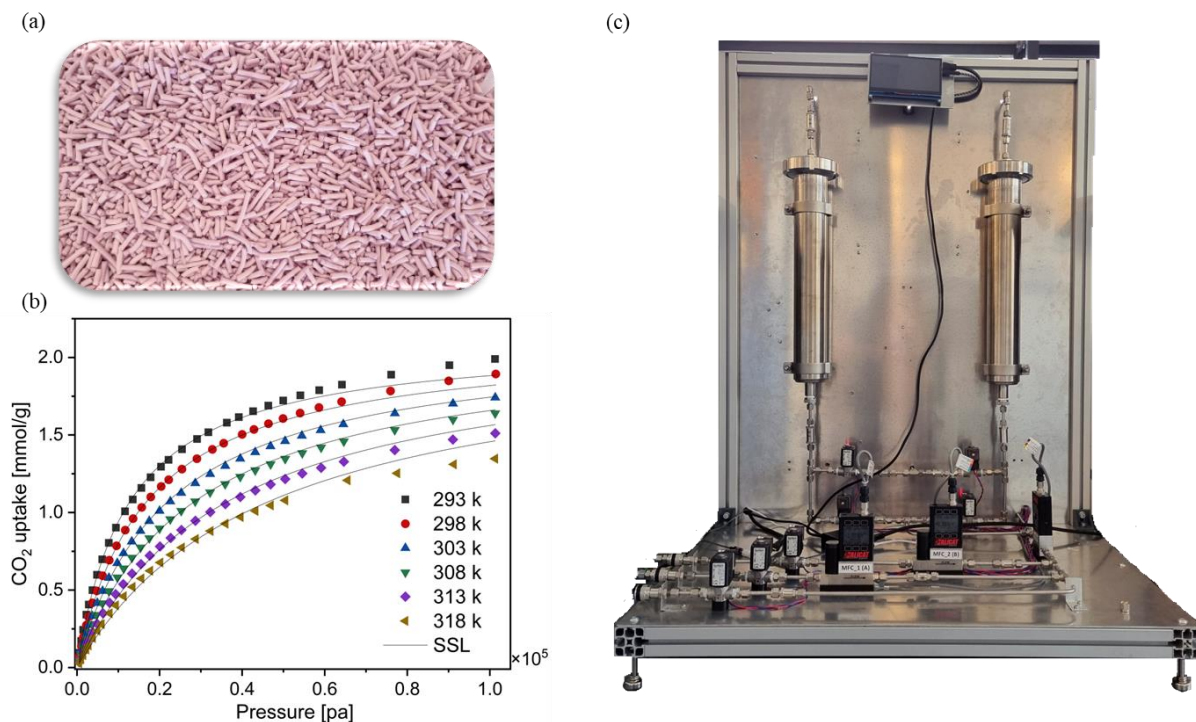| Parameter	Single-site Langmuir	
	CO_2	N_2
q^{sat} [mol kg^{-1}]	2.12	2.12
b_0 [1/pa]	6.15×10^{-12}	8.30×10^{-11}
$-\Delta U$ [kJ mol^{-1}]	39.89	20.37

(a)

(b)

(c)

Figure 1.(a) MUF-16 pellets; (b) CO_2 adsorption isotherms at various temperatures together with the single-site Langmuir fits; (c) a mobile rig with 2 kg of MUF-16 used for on-site industrial trials.

Next, we determined the behaviour under gas mixtures to account for any competition for the gases for the adsorption sites as well as the potential for cross-adsorbate interactions. Equilibrium adsorption data for binary gas mixtures can be defined by simplified models [21]. In this study, the Extended Langmuir model (Eq. 2) appropriately describes competitive CO_2 and N_2 co-adsorption from mixtures. This model uses the parameters obtained from the fittings for the isotherms of each component (i) [20].

$$q_i^* = \frac{q_i^{sat} b_i p_i}{1 + \sum b_i p_i} \tag{2}$$

where q_i^* is the solid equilibrium loading of component i, p_i is the partial pressure of component i, q_i^{sat} is the solid phase saturation capacity, b_i is the affinity parameter. The temperature dependence of the affinity parameter is described by Eq. 3:

$$b_i = b_{0,i} e^{-\Delta U_i / RT} \tag{3}$$

2.3. Process design and modeling

A computational model combined was developed in MATLAB to simulate and optimize the VSA processes. This work applies multi-objective optimization based on a genetic algorithm to create Pareto fronts. Three different VSA cycles (three-step, four-step, and five-step cycle) for post-combustion carbon capture applications were employed. Typical CO_2 flue gas compositions found in coal (15% CO_2) is employed first to compare these cycles together. Since the temperature and pressure in the column change during the PSA cycle, we used a non-isothermal and non-isobaric model. The code was validated with experimental data measured on a mobile PVSA rig filled with 1 kg of MUF-16 in each column. The breakthrough curve obtained by the developed model was compared with the experimental data under the same conditions in terms of the CO_2 concentration at the outlet of the adsorption column. Pleasingly, the simulation results are consistent with the experimental data, which shows that the mathematical model can accurately describe the actual adsorption process (Fig. 2).
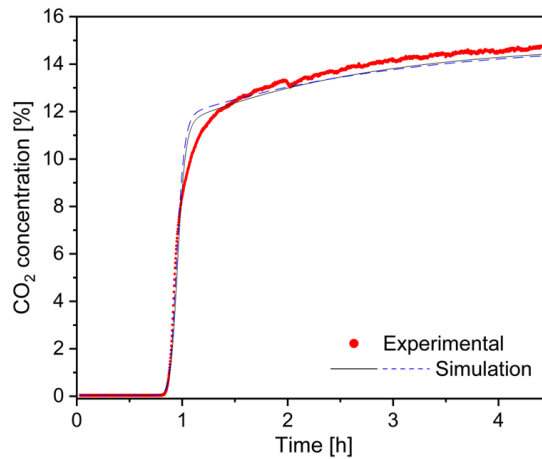

Figure. 2. Experimental and simulated breakthrough curves for 15/85 mixture of CO_2/N_2. The experimental data was obtained using a column filled with 1 kg of pelletised MUF-16 adsorbent,

For all three cycles, key variables such as feed composition, the length of the bed (1m), the inner diameter (14.45cm), the adsorption pressure (1bar) and the vacuum pressure (0.025 bar) were fixed and all optimization studies were conducted using identical ranges for the decision variables, as outlined in Table 2. The achievable separation performance will vary whenever any of these variables are changed. Optimization constraints are considered to ensure that the two adsorption columns operate in a way that maintains continuous flow throughout the process. The feed to the process was assumed to be a dry gas with flowrate of 50 Nm^3/h consisting only of CO_2 and N_2 at 1atm pressure and 25 °C.

Table 2. Bounds on the decision variables used to optimize MUF-16 studied in this work.

	t_{ADS} [s]	t_{EVAC} [s]	t_{BD} [s]	t_{HR} [s]	P_{BD} [bar]	$ß^*$ [-]
Lower bound	40	30	5	5	0.1	0.01
Upper bound	600	600	100	100	0.99	0.9

*ß: heavy reflux ratio

We first examined a very simple cycle composed of only three basic steps: pressurization, adsorption, and counter-current evacuation (Fig. 3a). As typically observed elsewhere, a three-step process was not able to meet the DOE targets for CO_2 purity and recovery [22]. Next, we considered a 4-step cycle by adding a co-current blowdown step (Fig. 3b). This is a simple, industrially-relevant VSA cycle with a long history. Finally, we considered a heavy reflux step, which is often important to attain CO_2 purity and recovery targets [23]. Thus, we developed a more complex five-step cycle (Fig. 3c) comprising a pressurization step, adsorption step, heavy reflux step, co-current blowdown step, and a counter-current evacuation step [22].

The most important criteria in swing adsorption processes are the CO_2 purity and recovery. Maximising these two parameters is the general objective of CO_2 separation processes, however trade-offs exist. Purity is given by the moles of CO_2 exiting during the evacuation step divided by the total number of moles of CO_2 and N_2 exiting during the evacuation step and recovery is the moles of CO_2 collected during evacuation divided by the moles of CO_2 introduced during the pressurisation and the adsorption steps. Swing adsorption processes for CO_2 capture should ideally meet the requirements of CCS (95% CO_2 purity and 90% CO_2 recovery), which was specified by the US Department of Energy (DOE) [24]. Here, optimisation was carried out to maximise purity and recovery.

For a more useful performance analysis, the estimation of CO_2 productivity and energy consumption is also essential. Productivity gives information about how quickly a product can be produced and how much adsorbent is required. The productivity is simply defined as the amount of CO_2 produced by a given amount of adsorbent over the course of one cycle [8]. The energy requirement is another important parameter in selecting the best adsorption process, which has a direct impact on the overall cost. In adsorption processes, most of the power is consumed by vacuum pumps, compressors and blowers[25]. Here, relative energies are presented rather than absolute energies. Finally, the feed composition, which is reflective of the different scenarios for the implementation of CCS, is an important consideration.

3. Results

3.1. Impact of different VSA cycles

Three different VSA cycles (three-step, four-step, and five-step cycle) for post combustion carbon capture applications were employed. A large number of solutions were found, which define Pareto fronts when comparing important outputs (Fig. 4). Foremost, both purity and recovery improve when the complexity of the cycle is increased (Fig. 4a). While the 3-step cycle is a basic adsorption process that is not well suited for practical carbon capture applications, we started with this cycle to systematically address how adding new steps can increase performance. Including a co-current blowdown step helps to remove N_2 from free spaces between the adsorbent pellets in column to increase the CO_2 purity. In this 4-step case, CO_2 purity exceeds 95%, as envisaged, although the maximum recovery simultaneously achievable is only ~65%. It is worth noting that it is possible to achieve higher purity and recovery in 4-step if the range of decision variables is changed or the adsorption pressure is increased (i.e. a pressure-vacuum swing adsorption process is used).
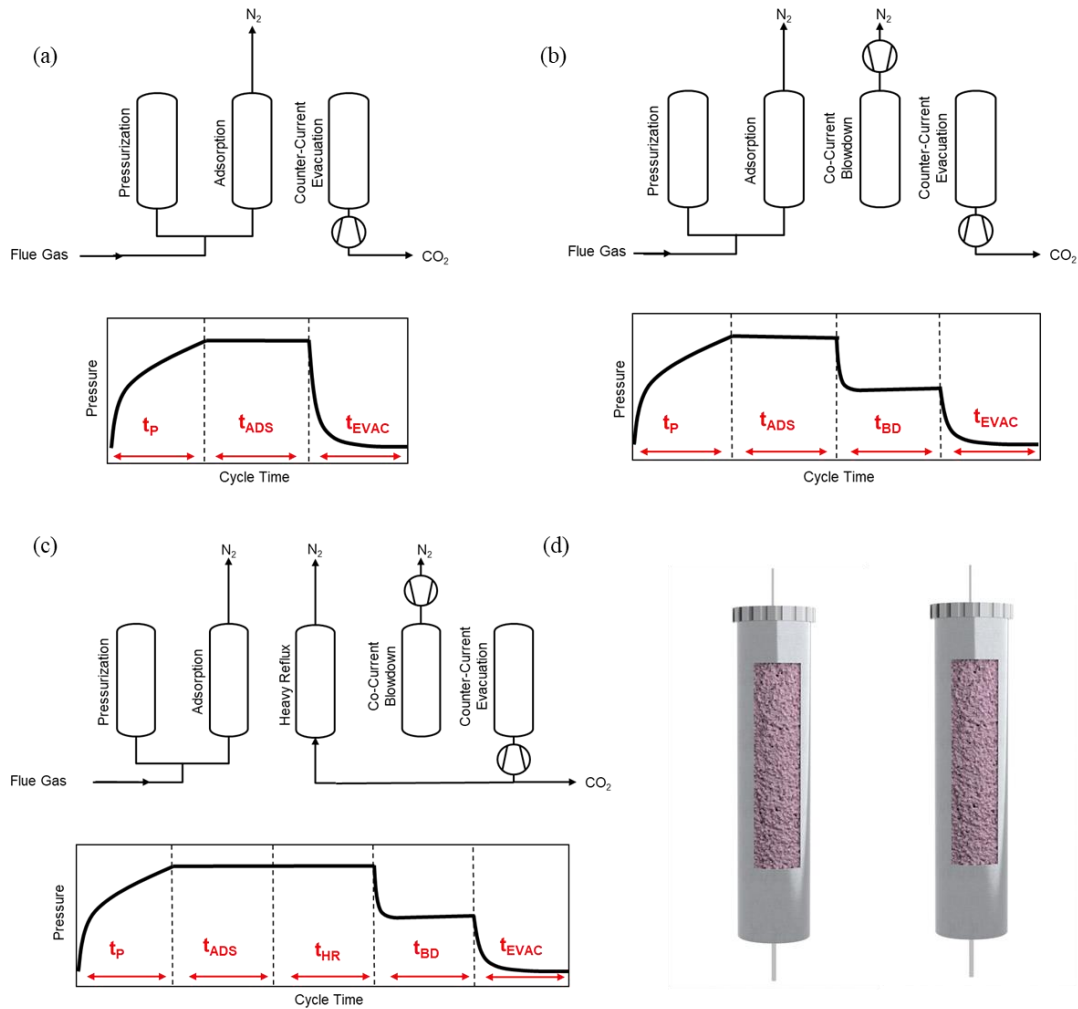
Figure 3. Process schematics of the three cycles tested in this work along with the pressure evolution over time: (a) Three-step cycle; (b) Four-step cycle; (c) Five-step cycle; (d) two-column VSA process

Our final case study is a five-step VSA cycle. In the adsorption step, operated at the high pressure (P_{ADS}), the feed enters the column at the bottom while bulk of the N_2 leaves the column at top. The main aim of this step is to adsorb the CO_2 within the column. At the end of the adsorption step, the column contains both CO_2 and N_2. Heavy reflux step takes a portion of the heavy product gas from the low-pressure column during the CnC evacuation step. This heavy reflux step efficiently purges the light component from the void spaces in the column while simultaneously filling the column from the feed end with the heavy component. Also, it can increase the partial pressure of CO_2 in the column to drive further CO_2 adsorption so less CO_2 escapes with the non-adsorbed gas [26]. Moreover, higher CO_2 loading on the adsorbent means that regeneration could demand more energy or time. So, as we can see the energy increases in this case compared to 4-step process. In the CoC blowdown step, operated at an intermediate pressure (P_{BD}; $P_{BD} \leq P_{ADS}$), N_2 is removed from top using a vacuum pump. The aim of this step is to remove enough N_2 so that high purity CO_2 product can be recovered in the subsequent step. The operating pressure, P_{BD}, is a critical operating variable. A high value results in low product purity and a low P_{BD} can result in a lower CO_2 recovery. In the evacuation step, operated at P_{EVAC} ($P_{EVAC} \leq P_{BD}$), CO_2 product is obtained by evacuating the column from the feed-end. The low pressure is often dictated by the pressure achievable by a vacuum pump. In the final step, feed is used to pressurize the column from bottom. With 5-step cycle process, we can simultaneously reach high purity and recovery, which shows that MUF-16 can be used on large scale with relatively simple process to purify CO_2 from flue gases.

Figure 4b, and c shows the energy-recovery/ productivity Pareto front for 4-step and 5-step cycle process, all points here satisfied a purity higher than 95%. The results show that energy consumption for CO_2 capture with purity more than 95% is modest. The achievable minimum energy for the four-step process is around 150 $kWh_e/tonne_{CO_2}$ at maximum recovery and productivity and around 230 $kWh_e/tonne_{CO_2}$ for 5-step to meet requirements. This result demonstrates that using MUF-16 in VSA is energetically favourable as it offers lower energy consumption compared to absorption process where the energy consumption is generally around 250 $kWh_e/tonne_{CO_2}$[27, 28].
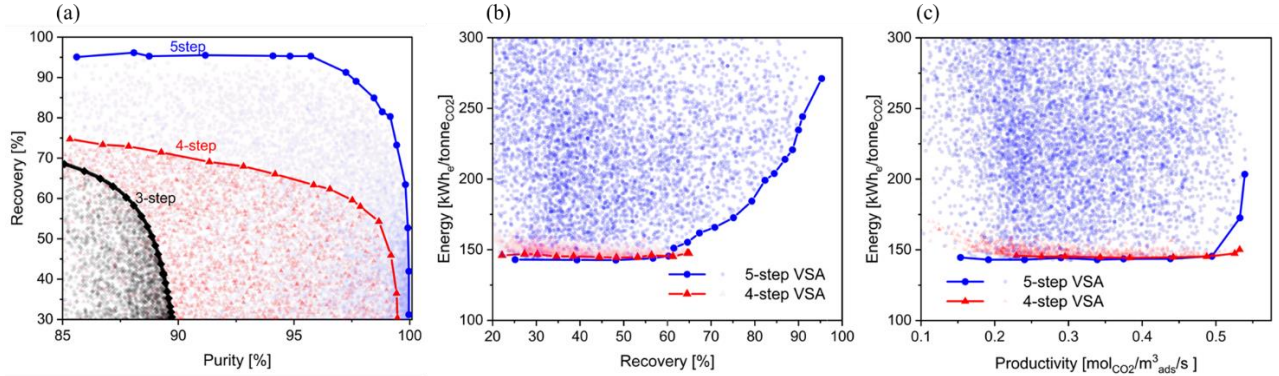

Figure 4. (a) Purity-recovery Pareto fronts for MUF-16 using 3-, 4- or 5-step VSA processes; (b, c) energy-recovery Pareto curves for 4- and 5-step processes. All points on the Pareto curves in panels (b) and (c) satisfy ≥ 95% purity. All energy values should be taken as relative, rather than absolute, values. They were calculated using a fixed vacuum pump efficiency of 72%.

A comparison was conducted between the VSA process results for MUF-16 and those for zeolite 13X and UTSA-16, as reported in the literature [29] assuming adsorption columns of the same size and a flue gas comprising 15% CO_2. The results indicate that that MUF-16 outperforms these other adsorbents when examined holistically[†].

Table 3. Process performance indicators for MUF-16, zeolite 13X and UTSA-16.

Parameter	UTSA-16 [29]	zeolite 13X [29]	MUF-16
P_{BD} [bar]	0.164	0.129	0.402
P_{EVAC} [bar]	0.024	0.018	0.025
v_0 [m/s]	0.426	0.620	2.290
Purity [%]	95.0	95.0	95.2
Recovery [%]	90.0	90.5	91.5
Productivity [$mol_{CO2}/m^3_{ads}/s$]	0.532	0.562	0.526

3.2. Impact of the feed composition (y)

Up to this point, our analysis has focused on a feed gas composition of 15% CO_2, which closely resembles the flue gas emitted from coal power plants. However, it is important to investigate whether the promising results from the 5-step cycle are also observed across a range of feed compositions. To evaluate the sensitivity of CO_2 capture performance to varying feed concentrations, simulations were conducted with CO_2 concentrations (y) ranging from 8% to 20%, while maintaining constant feed temperature, flow rate, evacuation pressure, and range of decision variables. A concentration of 8% CO_2 represents flue gas from natural gas power plants, whereas 20% CO_2 is typical of exhaust streams from cement production [29, 30]. We examined the effects of feed composition on purity, recovery, productivity, and energy consumption for the 5-step cycle (Fig. 5). At y = 8%, the current cycle and decision variable

---

[†] We note that this comparison is not a direct one-to-one evaluation due to variations in cycle times, decision variables, and process configurations across the referenced studies. However, the purpose of this analysis is to highlight the high performance of MUF-16 in effectively capturing CO_2 from flue gas. While the results are extremely promising, further research is necessary to conduct a comprehensive comparison of these adsorbents, particularly in terms of energy efficiency and cost-effectiveness.

range do not allow for recovery rates exceeding 88% while maintaining purity levels above 95%. Increasing the recovery would require shorter heavy reflux and blowdown times, which are beyond the decision variable limits specified in the current study. However, for y = 15% and 20%, recovery rates above 90% are achievable within the same range of decision variables.

As expected, higher CO_2 feed compositions lead to reduced energy consumption and improved productivity (Fig. 5c) [29] and VSA offers opportunities to offer lower energy consumption compared to absorption-based processes [27]. For lower CO_2 feed compositions, the P_{BD} must be further reduced to have good performance, so the energy consumption increases to reach same recovery as other CO_2 composition.

It can also be seen that the range of change of energy with respect to recovery is wider for y = 8% (Fig. 5b). High purity and recovery can be achieved with low energy consumption for y = 15% and 20%. In contrast, the higher energy demands associated with capturing dilute CO_2 are evident for the y = 8% flue gas.
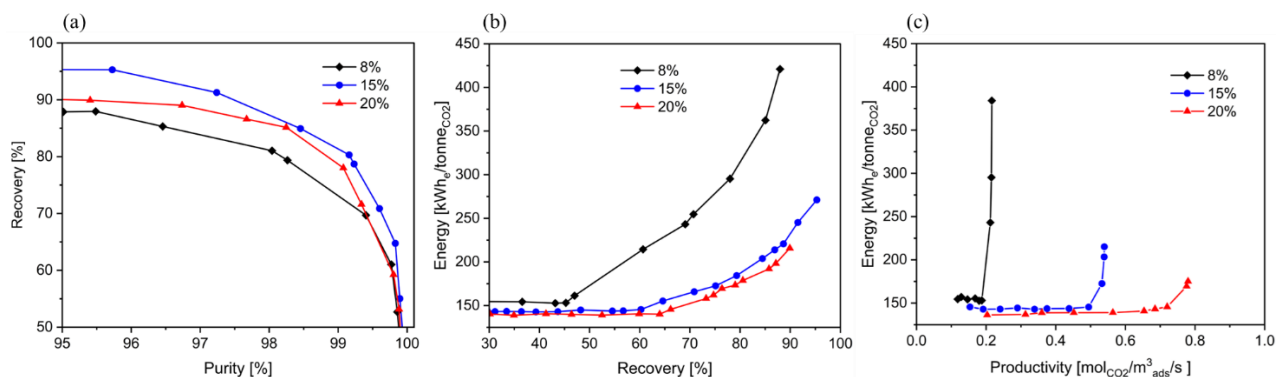

Figure 5. Impact of CO_2 levels in the flue gas, expressed as a percentage, on (a) Purity-recovery, (b) Energy-recovery, and (c) Energy-productivity Pareto curves using a five-step VSA process. All points on the Pareto curves (a), (b) and (c) satisfy ≥ 95% purity. All energy values should be taken as relative, rather than absolute, values. They were calculated using a fixed vacuum pump efficiency of 72%.

4. Conclusion

This study evaluates the performance of MUF-16 for VSA-based post-combustion CO_2 capture. A non-isothermal, and non-isobaric process simulator was coupled with a genetic algorithm to perform multi-objective optimizations. The results demonstrate that high CO_2 purities exceeding 95% can be achieved with both 4-step and 5-step cycles with low energy requirements, demonstrating the promise of MUF-16 for large-scale CO_2 capture using simple engineering processes. Furthermore, the findings confirm the versatility of MUF-16 for treating flue gases with various CO_2 concentrations. Further work will focus on PVSA simulations using MUF-16 to even further broaden its applicability.

Acknowledgements

References

1.   Raganati F, Ammendola P. CO2 Post-combustion Capture: A Critical Review of Current Technologies and Future Directions. Energy & Fuels. 2024;38(15):13858-905.
2.   Font-Palma C, Cann D, Udemu C. Review of Cryogenic Carbon Capture Innovations and Their Potential Applications. C. 2021;7(3):58.

3. Wang X, Song C. Carbon Capture From Flue Gas and the Atmosphere: A Perspective. Front Energy Res. 2020;8.

4. Zhang Y, Jangodaz E, Yin BH, Telfer SG. Functionalisation of MUF-15 enhances CO_2/CH_4 selectivity in mixed-matrix membranes. Chem Commun. 2024;60(46):5924-7.

5. Mohammad M, Isaifan RJ, Weldu Y, Rahman MA, Al-Ghamdi SG. Progress on carbon dioxide capture, storage and utilisation. Int J Global Warming. 2020.

6. Leung DYC, Caramanna G, Maroto-Valer MM. An overview of current status of carbon dioxide capture and storage technologies. Renewable Sustainable Energy Rev. 2014;39:426-43.

7. Soo XYD, Lee JJC, Wu W-Y, Tao L, Wang C, Zhu Q, et al. Advancements in CO_2 capture by absorption and adsorption: A comprehensive review. J CO_2 Util. 2024;81:102727.

8. Nguyen TTT, Shimizu GKH, Rajendran A. CO_2/N_2 separation by vacuum swing adsorption using a metal–organic framework, CALF-20: Multi-objective optimization and experimental validation. Chem Eng J. 2023;452:139550.

9. Rajendran A, Subraveti SG, Pai KN, Prasad V, Li Z. How Can (or Why Should) Process Engineering Aid the Screening and Discovery of Solid Sorbents for CO_2 Capture? Acc Chem Res. 2023;56(17):2354-65.

10. Rajagopalan AK, Rajendran A. The effect of nitrogen adsorption on vacuum swing adsorption based post-combustion CO_2 capture. Int J Greenhouse Gas Control. 2018;78:437-47.

11. Burns TD, Pai KN, Subraveti SG, Collins SP, Krykunov M, Rajendran A, et al. Prediction of MOF Performance in Vacuum Swing Adsorption Systems for Postcombustion CO_2 Capture Based on Integrated Molecular Simulations, Process Optimizations, and Machine Learning Models. Environmental Science & Technology. 2020;54(7):4536-44.

12. Sai Bhargava Reddy M, Ponnamma D, Sadasivuni KK, Kumar B, Abdullah AM. Carbon dioxide adsorption based on porous materials. RSC Adv. 2021;11(21):12658-81.

13. Zhang K, Wang R. A critical review on new and efficient adsorbents for CO_2 capture. Chem Eng J. 2024;485:149495.

14. Danaci D, Bui M, Mac Dowell N, Petit C. Exploring the limits of adsorption-based CO2 capture using MOFs with PVSA – from molecular design to process economics. Mol Syst Des Eng. 2020;5(1):212-31.

15. Zhang R, Shen Y, Tang Z, Li W, Zhang D. A Review of Numerical Research on the Pressure Swing Adsorption Process. Processes. 2022;10(5):812.

16. Qazvini OT, Babarao R, Telfer SG. Selective capture of carbon dioxide from hydrocarbons using a metal-organic framework. Nat Commun. 2021;12(1):197.

17. Qazvini OT, Telfer SG. MUF-16: A Robust Metal–Organic Framework for Pre- and Post-Combustion Carbon Dioxide Capture. ACS Appl Mater Interfaces. 2021;13(10):12141-8.

18. Trump BA, Qazvini OT, Lee SJ, Jangodaz E, Zhou W, Brown CM, et al. Flexing of a Metal–Organic Framework upon Hydrocarbon Adsorption: Atomic Level Insights from Neutron Scattering. Chem Mater. 2023;35(3):1387-94.

19. Campbell N, Telfer S, Lee S, Jangodaz E. MUF-16 for Point-Source Carbon Dioxide Capture. 17th Greenhouse Gas Control Technologies Conference (GHGT-17); 2024; Canada, Calgary: SSRN.

20. Nguyen TTT, Lin J-B, Shimizu GKH, Rajendran A. Separation of CO_2 and N_2 on a hydrophobic metal organic framework CALF-20. Chem Eng J. 2022;442:136263.

21. Hu Z, Wang Y, Shah BB, Zhao D. CO_2 Capture in Metal–Organic Framework Adsorbents: An Engineering Perspective. Adv Sustainable Syst. 2019;3(1):1800080.

22. Leperi KT, Yancy-Caballero D, Snurr RQ, You F. 110th Anniversary: Surrogate Models Based on Artificial Neural Networks To Simulate and Optimize Pressure Swing Adsorption Cycles for CO_2 Capture. Ind Eng Chem Res. 2019;58(39):18241-52.

23. Reynolds SP, Mehrotra A, Ebner AD, Ritter JA. Heavy reflux PSA cycles for CO_2 recovery from flue gas: Part I. Performance evaluation. Adsorption. 2008;14(2):399-413.

24. Jiang N, Shen Y, Liu B, Zhang D, Tang Z, Li G, et al. CO_2 capture from dry flue gas by means of VPSA, TSA and TVSA. J CO2 Util. 2020;35:153-68.

25. Zanco SE, Pérez-Calvo J-F, Gasós A, Cordiano B, Becattini V, Mazzotti M. Postcombustion CO_2 Capture: A Comparative Techno-Economic Assessment of Three Technologies Using a Solvent, an Adsorbent, and a Membrane. ACS Eng Au. 2021;1(1):50-72.

26. Ritter JA, Ebner AD, McIntyre JA, Reynolds SP, Gadre SA. Radically New Adsorption Cycles for Carbon Dioxide Sequestration. United States; 2005 2005-10-11.

27. Pai KN, Prasad V, Rajendran A. Practically Achievable Process Performance Limits for Pressure-Vacuum Swing Adsorption-Based Postcombustion CO_2 Capture. ACS Sustainable Chem Eng. 2021;9(10):3838-49.

28. Singh A, Stéphenne K. Shell Cansolv CO_2 capture technology: Achievement from First Commercial Plant. Energy Procedia.

2014;63:1678-85.
29. Maruyama RT, Pai KN, Subraveti SG, Rajendran A. Improving the performance of vacuum swing adsorption based CO_2 capture under reduced recovery requirements. Int J Greenhouse Gas Control. 2020;93:102902.
30. Biermann M, Normann F, Johnsson F, Skagestad R. Partial Carbon Capture by Absorption Cycle for Reduced Specific Capture Cost. Ind Eng Chem Res. 2018;57(45):15411-22.